THE UNIVERSITY OF

WARWICK

warwick**publications**wrap

highlight your research

http://wrap.warwick.ac.uk
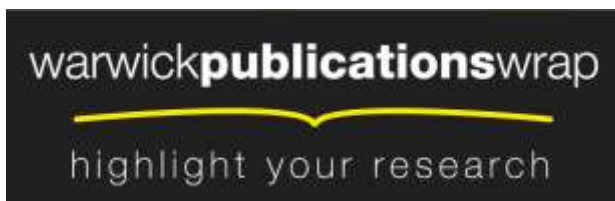
Fast particle-driven ion cyclotron emission (ICE) in tokamak plasmas and the case for an ICE diagnostic in ITER

K.G. McClements[1]**, R. D'Inca**[2]**, R.O. Dendy**[1,3]**, L. Carbajal**[3]**,**
S.C. Chapman[3]**, J.W.S. Cook**[3]**, R.W. Harvey**[4]**, W.W. Heidbrink**[5]
and S.D. Pinches[6]

[1] CCFE, Culham Science Centre, Abingdon, Oxfordshire OX14 3DB, UK
[2] Max-Planck-Institut für Plasmaphysik, Garching D-85748, Germany
[3] CFSA, Department of Physics, Warwick University, Coventry CV4 7AL, UK
[4] CompX, Del Mar, CA 92014-5672, USA
[5] University of California, Irvine, CA 92697, USA
[6] ITER Organization, Route de Vinon-sur-Verdon, CS 90 046, 13067 t Paul-lez-Durance
Cedex, France

E-mail: k.g.mcclements@ccfe.ac.uk

Abstract

The detection of fast particle-driven waves in the ion cyclotron frequency range (ion cyclotron emission or ICE) could provide a passive, non-invasive diagnostic of confined and escaping fast particles (fusion α-particles and beam ions) in ITER, and would be compatible with the high radiation environment of deuterium–tritium plasmas in that device. Recent experimental results from ASDEX Upgrade and DIII-D demonstrate the efficacy of ICE as a diagnostic of different fast ion species and of fast ion losses, while recent particle-in-cell (PIC) and hybrid simulations provide a more exact comparison with measured ICE spectra and open the prospect of exploiting ICE more fully as a fast ion diagnostic in future experiments. In particular the PIC/hybrid approach should soon make it possible to simulate the nonlinear physics of ICE in full toroidal geometry. Emission has been observed previously at a wide range of poloidal angles, so there is flexibility in the location of ICE detectors. Such a detector could be implemented in ITER by installing a small toroidally orientated loop near the plasma edge or by adding a detection capability to the ion cyclotron resonance heating (ICRH) antennae. In the latter case, the antenna could be used simultaneously to heat the plasma and detect ICE, provided that frequencies close to those of the ICRH source are strongly attenuated in the detection system using a suitable filter. Wavenumber information, providing additional constraints on the fast ion distribution exciting the emission, could be obtained by measuring ICE using a toroidally distributed array of detectors or different straps of the ICRH antenna.

Keywords: ion cyclotron emission, fusion alpha-particles, beam ions, ITER

(Some figures may appear in colour only in the online journal)

1. Introduction

Electromagnetic emission from magnetically confined plasmas in the ion cyclotron frequency range is generally categorized as ion cyclotron emission (ICE). This emission is invariably driven by ions that are superthermal but not necessarily super-Alfvénic; ICE from deuterium plasmas heated ohmically or by hydrogen beams was reported in the early years of JET

operation [1, 2]; here the emission intensity scaled with the deuterium–deuterium neutron rate and for this reason was attributed to the charged products of thermonuclear fusion reactions. ICE is usually detected using either an ion cyclotron resonance heating (ICRH) antenna in receiver mode or a dedicated radio frequency (RF) probe (loop or dipole). Fusion experiments in which emission identified as ICE has been detected include ASDEX Upgrade [3], DIII-D [4], JET [1, 2], JT-60U [5], LHD [6], PDX [7] and TFTR [8]. This is a passive, non-invasive diagnostic measurement that would be compatible with the high radiation environment of DT burning plasmas in ITER and could yield important information on
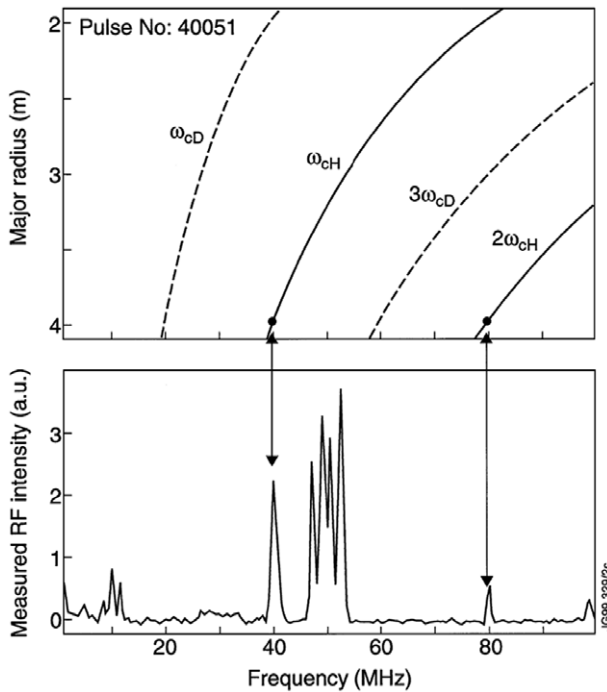
**Figure 1.** Lower plot: RF emission spectrum during four-frequency H minority ICRH in JET pulse 40051. ICE peaks corresponding to the H cyclotron frequency and its second harmonic in the outer plasma edge (indicated by the upper plot) can be seen. Reproduced with permission from [11]. Copyright 2000 by the American Physical Society.

the fusion α-particle and beam ion populations in that device, complementing other diagnostics such as collective Thomson scattering. In this paper we report on recent progress in the experimental (section 2) and theoretical (section 3) study of ICE, and present the case for an ICE diagnostic in ITER (section 4).

2. Observations of ICE

In the 1991 JET Preliminary Tritium Experiment (PTE), peaks in ICE intensity were observed in both pure deuterium and DT pulses at frequencies close to the α-particle/deuterium cyclotron frequency ω_{cD} in the outer midplane edge (17 MHz) and at cyclotron harmonics n up to $n = 10$ [9]; higher harmonics appeared to merge into a continuum. A linear relation was found between ICE intensity and neutron rate in JET over six orders of magnitude. The total ICE power measured using the JET ICRH antenna (a few μW at most) was many orders of magnitude smaller than the RF power P_{RF} (several MW) which the antenna was capable of launching into the plasma. ICE detected in the 1997 DT experiments in JET provided evidence of classical α-particle confinement [10].

ICE was also detected in JET using a dedicated probe mounted on the inner side of vacuum vessel, in particular during (H)D minority ICRH [11]. In these pulses the minority protons typically had a temperature perpendicular to the magnetic field of around 2 MeV. The lower plot in figure 1 shows the RF spectrum during a pulse with $P_{RF} = 5.6$ MW, in which four RF generators were tuned to frequencies clustered around 50 MHz. In addition to peaks associated with ICRH,
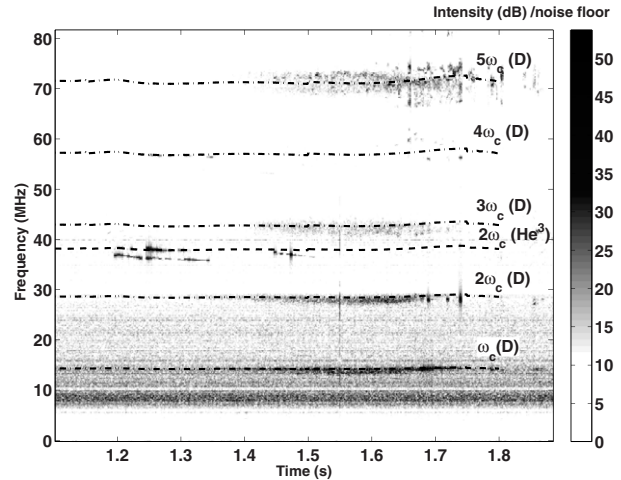

Figure 2. High field side spectrogram from ASDEX Upgrade discharge 26915, a D plasma with toroidal field 2.5 T, central density 6×10^{19} m^{-3} and NBI power 10 MW. The dashed lines indicate cyclotron harmonics of D/H and ^{3}He at normalized minor radius $r/a = 0.95a$.

two additional peaks corresponding to the hydrogen cyclotron frequency ω_{cH} and its second harmonic in the outer midplane (see upper plot) are clearly visible. A key point here is that the very large disparity between the transmitted and received RF power does not prevent ICE from being detected. More recently, ICE driven by ^{3}He minority fast ions (accelerated by ICRH) was detected using a sub-harmonic arc detection system on the JET ICRH antennas [12].

In recent years ICE has been observed in ASDEX Upgrade [3], DIII-D [4], JT-60U [5] and LHD [6]. In ASDEX Upgrade ICE is detected using a dedicated probe (consisting of two cross-dipole antennae) and a voltage probe inside the ICRH antenna on the high and low field sides of the plasma respectively. ICE has been observed at ω_{cD} in the plasma centre (plus its second and third harmonics) during deuterium NBI and at ω_{cH} in the outer plasma edge during minority hydrogen ICRH. In pulses with high power (> 5 MW) deuterium beam injection into deuterium target plasmas, transient ICE has been detected at the second harmonic of the ^{3}He cyclotron frequency in the plasma edge (probably driven by ^{3}He fusion products), along with longer lasting emission at several deuterium harmonics (figure 2). While ^{3}He fusion products are born with speeds v significantly greater than the Alfvén speed c_A in these plasmas, deuterium beam ions have v of the order of c_A or less, from which one may conclude that ICE does not require the fast ion population to be strongly super-Alfvénic. This was also found to be the case in TFTR [13].

In DIII-D a magnetic loop on the low field side [14] filters the ICE signal into a lower band, which includes ω_{cD} at the plasma edge, and a higher band which covers $2\omega_{cD}$ and $3\omega_{cD}$ (figure 3). Bursting beam ion-driven ICE is observed in both frequency bands during the excitation of off-axis fishbone modes, whose eigenfunctions are localized in the plasma core region, peaking near the magnetic flux surface with safety factor $q = 2$ [4]. The envelope of the ICE is observed to rise and decay with the fishbone amplitude; within this envelope, the ICE undergoes large amplitude fluctuations with a frequency close to that of the fishbone itself. In the case of the
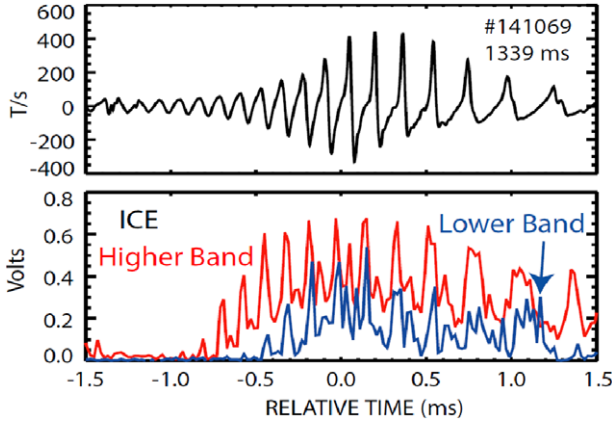
Figure 3. Mirnov coil signal (top) and ICE signals in two frequency bands (bottom) during fishbone in DIII-D. The lower and higher bands include, respectively, the deuterium cyclotron frequency at the plasma edge and the second and third harmonics of this [4]. © IOP Publishing. Reproduced by permission from IOP Publishing. All rights reserved.

higher band emission, the time of peak ICE intensity coincides with that of the fishbone amplitude (within experimental error). ICE in DIII-D is found to be correlated more strongly with drops in neutron flux during fishbone excitation than are signals from more direct measurements of beam ion losses. The interpretation of this result is that the ICE is driven by a two-step process in which the fishbones expel beam ions from the plasma core region to the edge, where they excite ICE eigenmodes. As in other conventional tokamaks, the beam ions in DIII-D are sub-Alfvénic.

3. Interpretation of ICE

ICE is generally attributed to the magnetoacoustic cyclotron instability (MCI), which results from the resonant interaction of energetic ions with fast Alfvén waves [15]. Instability can be driven by anisotropy, population inversion perpendicular to the magnetic field or radial gradients. In the case of JET, inverted fusion α-particle distributions of the type required to drive ICE arose in the outer midplane plasma edge due to the large radial excursions from the core to the edge of marginally trapped particles [9]. The local α-particle distribution in the outer midplane f_α was dominated by particles originating from the plasma core, and consequently had a bump-in-tail determined by the fusion reaction rate in the core and the usual constants of motion. Waves propagating obliquely with respect to the magnetic field $\boldsymbol{B}$ have been shown to be linearly unstable when the energetic ion concentration is very low, due to the Doppler shift term in the cyclotron resonance condition causing thermal cyclotron damping to be decoupled from the drive. Nevertheless the growth rates in a uniform equilibrium plasma are typically found to peak at propagation angles that are nearly perpendicular to $\boldsymbol{B}$ [15]. The inclusion of grad-B and curvature drift terms in the cyclotron resonance condition leads to prediction of higher growth rates, and the maximum drive is again found for nearly perpendicular propagation [16]. Toroidal effects on the linear stability of these modes are discussed further in [17]. Generally, it is found that the linear drive falls off fairly rapidly (but remains finite) as the energetic
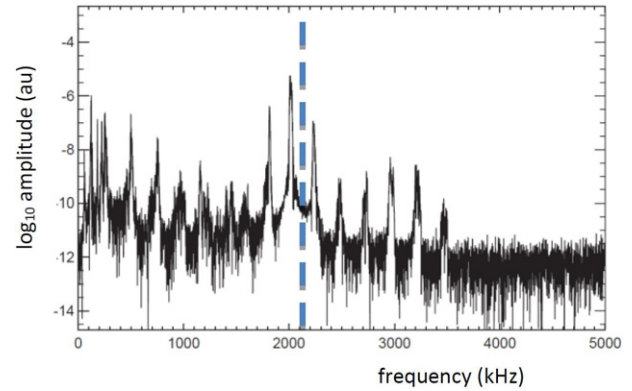
ion distribution broadens or the Alfvénic Mach number falls below one.

It should be noted that there is no essential physical difference between ICE eigenmodes and compressional Alfvén eigenmodes (CAEs) in the ion cyclotron frequency range, which have been observed in both spherical [18, 19] and conventional [20] tokamaks and, like ICE, have been attributed to fast Alfvén waves driven unstable due to cyclotron resonances with energetic ions. The close connection between ICE and CAEs is particularly illustrated by recent experiments at low toroidal magnetic field in the MAST spherical tokamak, where multiple CAEs were excited by deuterium beam ions in the ion cyclotron range [19]. In the spectrum shown in figure 4, three peaks occurring at frequencies close to ω_{cD} (evaluated at the magnetic axis) have amplitudes exceeding those of neighbouring peaks by a factor of 10^2 or more.

The identification of ICE (and CAEs) with fast Alfvén waves has prompted several investigations of the global structure of these modes in tokamak geometry. Gorelenkov and Cheng [21] developed an analytical theory of fast Alfvén eigenmode structure for circular cross-section, finite aspect ratio cold plasmas. The modes were found to be localised radially to minor radii $r = r_0$ such that

$$\frac{r_0^2}{a^2} = \frac{1}{1+\sigma} - (2s+1)\frac{\sqrt{2\sigma/(1+\sigma)}}{m(1+\sigma)}, \qquad (1)$$

where m, s are poloidal and radial mode numbers, and σ is a parameter controlling the density profile $n(r)$:

$$n(r) = n_0 \left(1 - r^2/a^2\right)^\sigma. \qquad (2)$$

For flat profiles ($\sigma < 1$), ICE eigenmodes are thus predicted to be localized near the plasma edge. However eigenfunctions of modes in the ion cyclotron range computed numerically by Smith and Verwichte [22] for a range of plasma shapes (but still using a cold plasma model) have a more extended radial structure.

There has been significant recent progress in the nonlinear modelling of ICE [23, 24]. Particle-in-cell (PIC) simulations with one space and three velocity dimensions have been used, for the first time, to study self-consistently the excitation of the MCI by a population-inverted fast ion distribution and the subsequent relaxation of this distribution [23]. Specifically,

Figure 4. Spectrum of fluctuations measured using Mirnov coil in deuterium beam-heated MAST pulse 27147. The dashed line indicates $\omega_{cD}/2\pi$ at the magnetic axis [19].
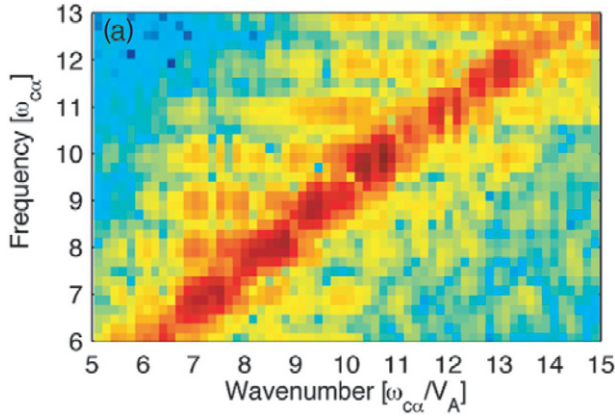
Figure 5. Wavenumber–frequency plot for the oscillatory component of B in a PIC simulation of the MCI, showing excitation of multiple α-particle cyclotron harmonics [23]. © IOP Publishing. Reproduced by permission of IOP Publishing. All rights reserved.

the initial fast ion distribution (α-particles) was modelled as a monoenergetic gyrotropic ring. Fourier analysis of the results in the space and time domains indicates linear dispersion, with the ratio of wave frequency ω to wavenumber k close to c_A (figure 5). Since the plasma beta is very low and wave propagation is necessarily perpendicular to the magnetic field in this simulation, it may be inferred that the excited waves are on the fast Alfvén branch. It is also apparent from figure 5 that the wave amplitude has local maxima (indicated in dark red) at frequencies close to harmonics of the α-particle cyclotron frequency, $\omega_{c\alpha}$. Hybrid simulations, again in one space dimension, which track full orbits of ions and treat electrons as a neutralizing fluid, have been used to explore the later stages of the MCI [24], thereby providing a more exact comparison with measured ICE spectra and opening the prospect of exploiting more fully this emission process as a fast ion diagnostic. The initial fast ion distribution was again modelled as a monoenergetic gyrotropic ring. In simulations with parameters close to those of the PTE in JET, the nonlinearly saturated ICE amplitude was found to depend strongly on the fast ion concentration ξ at low cyclotron harmonics, but only weakly on ξ at high harmonics: see figure 6(*b*). For realistic ξ the nonlinearly saturated spectrum (figure 6(*c*)) closely resembles the measured one (figure 6(*a*)). Using this hybrid approach in combination with a finite orbit width Fokker–Planck code such as CQL3D to generate realistic fast ion distributions [25], it will soon become possible to simulate nonlinearly ICE in full toroidal geometry.

A possible role for toroidal effects in determining ICE spectra is suggested by the fact that the high harmonic ICE peaks in the measured spectrum shown in figure 6(*a*) appear to merge into a continuum. This merging has been attributed to grad-B and curvature drift modifications to the wave–particle resonance condition, which would have the effect of splitting the ICE lines into doublets, with components merging into each other at high mode number and hence high frequency [9]. However drift effects were not included in the PIC and hybrid simulations reported in [23, 24], since uniform plasma equilibria were used, and indeed the high harmonic ICE peaks do not merge into a continuum in the simulations (figure 6(*c*)).
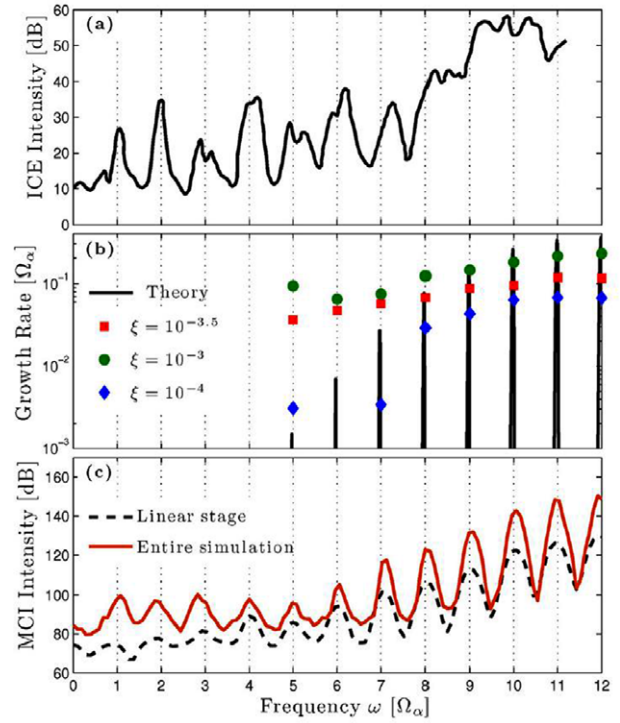
Figure 6. (*a*) Measured ICE spectrum in JET DT pulse 26148. (*b*) MCI linear growth rates from analytical theory (for $\xi = 10^{-3}$: black curve) and hybrid simulations (for three values of ξ: coloured points). (*c*) B_z intensity in linear (dashed curve) and nonlinear (solid curve) stages of instability in hybrid simulation with $\xi = 10^{-3}$. Reprinted with permission from [24]. Copyright 2014, AIP Publishing LLC.

4. Excitation and detection of ICE in ITER plasmas

As an illustrative example, we consider an ITER plasma in the baseline inductive mode of operation with toroidal field $B_0 = 5.3$ T, electron density $n_e = 10^{20}$ m^{-3}, equal concentrations of deuterium and tritium, 2% helium, 2% beryllium and 0.1% argon [26]. In this case the Alfvén speed c_A will be approximately $(5–6) \times 10^6$ m s^{-1} on the low field side of the plasma. As noted previously, ICE can be strongly driven by ions with speeds v in excess of c_A. Depending on velocity-space gradients, fusion α-particles and 1 MeV beam deuterons, born respectively with $v = 1.3 \times 10^7$ m s^{-1} and $v = 10^7$ m s^{-1}, are thus expected to provide strong drive for ICE in ITER, particularly since they will have much higher densities than α-particles in JET DT plasmas. However, compared to JET or TFTR, fusion α-particles in ITER will have smaller orbits relative to the machine size and, in the absence of significant levels of non-classical transport, will be better confined; beam ions are also expected to be well-confined. Centrally born trapped fusion α-particles will have a potato orbit width Δ_α given by [10].

$$\frac{\Delta_\alpha}{a} \approx 8.8 \left(\frac{a}{R}\right)^{1/3} \left(\frac{m_\alpha v}{Z_\alpha e \mu_0 I_p}\right)^{2/3}, \qquad (3)$$

where R and a are major and minor radii, m_α and $Z_\alpha e$ are the α-particle mass and charge, I_p is the plasma current and μ_0 is free space permeability. This expression yields $\Delta_\alpha = 0.4a$

and 0.5a for $I_\mathrm{p} = 15$ MA and 10 MA respectively. Trapped α-particles born further out will have a maximum orbit width [27]

$$\frac{\Delta_\alpha}{a} \approx \frac{a}{(Rr)^{1/2}} \frac{2\pi m_\alpha v}{Z_\alpha e \mu_0 I_\mathrm{p}}. \tag{4}$$

When $r = a/2$ this expression gives $\Delta_\alpha = 0.07a$ and $0.1a$ for $I_\mathrm{p} = 15$ MA and 10 MA. Given that the α-particle density profile n_α in both scenarios is predicted to be strongly peaked in the plasma centre, it may be inferred from these estimates that ring-like energetic ion distributions of the type believed to have driven ICE in JET are unlikely to be found in the ITER edge plasma under steady-state conditions, although they could arise deeper inside the plasma, depending on how steeply n_α falls off with radius.

The steady-state excitation of ICE in ITER would depend also on the structure of the corresponding Alfvén eigenmodes, and, if excited deep inside the plasma, it is unclear that ICE could propagate to a detector without being strongly absorbed *en route*, for example due to the ion–ion hybrid resonances that exist in DT plasmas [28]. However, even if detectable levels of ICE are not normally produced in steady-state conditions in ITER, it is likely that it could be used as an additional method of studying fast ion redistribution and losses resulting from MHD activity. As noted previously, ICE eigenmodes have been predicted to be localized to the outer region of the plasma, and ICE could thus be excited by a transient flux of fast particles being ejected from the plasma core due to MHD events. In addition to the correlations between ICE and fishbones observed in DIII-D [4], clear evidence has also been found of links between this type of emission and both sawteeth and edge localized modes in JET [9] and with toroidal Alfvén eigenmodes in LHD [6]. The detection of ICE in ITER would provide information on energetic ion behaviour supplementing that obtained using other diagnostics, such as collective Thomson scattering and γ-ray detectors. It should be noted that the heat loads in the DT phase of ITER operation will make it impossible to use a conventional fast ion loss detector unless a reciprocating drive system is used [29]. ICE detection could provide an alternative method of studying α-particle and beam ion losses.

In principle detection of ICE is possible using any technique for measuring magnetic, electric or density fluctuations in the ion cyclotron range. Dedicated RF probes have been used at a wide range of poloidal locations, for example at the top of the vessel in TFTR [30] and the high field side in JET [11]. The design requirements of an ICE diagnostic system for ITER are thus flexible. Other detection possibilities include microwave reflectometry, which is planned for ITER [31] and has been used to measure the spatial structure of modes at frequencies up to the CAE range in NSTX [32]; this is not a passive technique, however, since it requires microwaves to be launched into the plasma. Generally, ICE detection in existing devices is a passive, non-invasive diagnostic technique. It should be fully compatible with the high radiation environment of DT operation in ITER. For a dedicated diagnostic, the detector could be a modified plasma-facing component, as in DIII-D [14]; this works well for modes with predominately compressional polarization, such as ICE. If possible, the detector should be capable of detecting frequencies ranging up to around the tenth harmonic of the α-particle cyclotron

frequency, i.e. several hundred MHz. It would be particularly useful to have a toroidally distributed array of detectors, since this would provide wavevector information as well as spectra and thereby provide additional information on the fast ion distribution that is exciting the emission. ICE measurements in JET and ASDEX Upgrade show that a dedicated ICE probe can operate well during ICRH [3, 11], in particular that the ICE signal can be clearly distinguished from that due to the ICRH source, despite the very large disparity noted previously between ICRH power coupled to the plasma and the measured power in ICE.

Alternatively, or in addition to a dedicated diagnostic, a detection capability could be added to the ITER ICRH antenna system (for a technical description of this system, see [33]). ICE measurements could be carried out with the antenna in passive reception mode, as in the JET PTE experiment [9]. However the recent measurements in ASDEX Upgrade [3] demonstrate that it is also possible to detect emission with ICRH antennae during active operation of the same antennae for plasma heating: this in fact was how ICE in ASDEX Upgrade was first observed, with a probe located inside the ICRH transmission line. For this system to work it was necessary to ensure that the probe was located near a maximum voltage point of the standing wave pattern in the transmission line. The frequency of the ICRH source needed to be eliminated from the signal using a filter, with strong attenuation in a narrow bandwidth around the rejected frequency. A low-noise amplifier was also required to extract the ICE signal from the background. In a future system of this type on ITER, wavevector information could be determined by comparing the phase of the emission in different straps of the ICRH antennae; as noted above, such measurements are likely to enhance significantly the utility of ICE as a fast particle diagnostic. On ASDEX Upgrade it was found that measurements obtained using the dedicated ICE probe had a somewhat better signal-to-noise ratio than those obtained using the probe in the ICRH system.

5. Summary

ICE was used to obtain valuable information on the behaviour of fusion α-particles in the two large tokamaks capable so far of DT operation (JET and TFTR), and continues to be a useful diagnostic of confined and escaping fast ions in many fusion experiments. This is a passive, non-invasive diagnostic that would be compatible with the high radiation environment of DT plasmas in ITER, and could thus provide a valuable additional route to the experimental study of fusion α-particles and beam ions in that device. In JET, ICE from confined fusion products scaled linearly with the fusion reaction rate over six orders of magnitude, and provided evidence that α-particle confinement was close to classical. More recently, the intensity of beam-driven ICE in DIII-D has been found to be more strongly correlated with drops in neutron rate during fishbone excitation than are signals from more direct beam ion loss diagnostics. ICE in ASDEX Upgrade has been observed to be excited by both super-Alfvénic DD fusion products and sub-Alfvénic deuterium beam ions. The MCI, driven by the resonant interaction of population-inverted energetic ions with fast Alfvén waves, provides a credible explanation for ICE. PIC

and hybrid simulations have been used to explore the nonlinear stage of the MCI, thereby providing a more exact comparison with measured ICE spectra and opening the prospect of exploiting ICE more fully as a fast ion diagnostic; it should soon become possible to simulate nonlinear physics of ICE in full toroidal geometry. Emission has been observed at a wide range of poloidal locations, so there is considerable flexibility in the requirements of an ICE detector. Such a system could be implemented in ITER by installing a dedicated probe, for example a magnetic loop, or by adding a detection capability to the ICRH antenna system. In the latter case measurements on ASDEX Upgrade demonstrate the feasibility of using antennae simultaneously to heat plasma and to detect ICE.

Acknowledgments

References

[1] Cottrell G.A. *et al* 1986 *Proc. 13th EPS Conf. on Controlled Fusion Plasma Heating (Schliersee, Germany, 1986)* vol 2, p 37

[2] Cottrell G.A. and Dendy R.O. 1988 *Phys. Rev. Lett.* **60** 33

[3] D'Inca R. *et al* 2011 *Proc. 38th EPS Conf. on Plasma Physics (Strasbourg, France, 2011)* P1.053 http://ocs.ciemat.es/EPS2011PAP/pdf/P1.053.pdf

[4] Heidbrink W.W. *et al* 2011 *Plasma Phys. Control. Fusion* **53** 085028

[5] Ichimura M. *et al* 2008 *Nucl. Fusion* **48** 035012

[6] Saito K. *et al* 2013 *Plasma Sci. Technol.* **15** 209

[7] Heidbrink W.W. and Sadler G.J. 1994 *Nucl. Fusion* **34** 535

[8] Zweben S.J. *et al* 2000 *Nucl. Fusion* **40** 91

[9] Cottrell G.A. *et al* 1993 *Nucl. Fusion* **33** 1365

[10] McClements K.G. *et al* 1999 *Phys. Rev. Lett.* **82** 2099

[11] Cottrell G.A. 2000 *Phys. Rev. Lett.* **84** 2397

[12] Jacquet P. *et al* 2011 *AIP Conf. Proc.* **1406** 17

[13] Dendy R.O. *et al* 1994 *Phys. Plasmas* **1** 3407

[14] Watson G. and Heidbrink W.W. 2003 *Rev. Sci. Instrum.* **74** 1605

[15] Dendy R.O. *et al* 1994 *Phys. Plasmas* **1** 1918

[16] Fülöp T. and Lisak M. 1998 *Nucl. Fusion* **38** 761

[17] Hellsten T. *et al* 2006 *Nucl. Fusion* **46** S442

[18] Gorelenkov N.N. *et al* 2002 *Nucl. Fusion* **42** 977

[19] Sharapov S.E. *et al* 2014 *Phys. Plasmas* **21** 082501

[20] Heidbrink W.W. *et al* 2006 *Nucl. Fusion* **46** 324

[21] Gorelenkov N.N. and Cheng C.Z. 1995 *Nucl. Fusion* **35** 1743

[22] Smith H.M. and Verwichte E. 2009 *Plasma Phys. Control. Fusion* **51** 075001

[23] Cook J.W.S. *et al* 2013 *Plasma Phys. Control. Fusion* **55** 065003

[24] Carbajal L. *et al* 2014 *Phys. Plasmas* **21** 012106

[25] Harvey R.W. *et al* 2014 *Proc. 25th IAEA Fusion Energy Conf. (St. Petersburg, Russia, 2014)* TH/P6-49 http://www-pub.iaea.org/MTCD/Meetings/PDFplus/2014/cn221/cn221ConferenceProgrammeAndAbstracts.pdf

[26] Polevoi A.R. *et al* 2006 *Plasma Phys. Control. Fusion* **48** A449

[27] Kadomtsev B.B. and Pogutse O.P. 1967 *Sov. Phys.—JETP* **24** 1172

[28] Lilley M.K. and Sharapov S.E. 2007 *Phys. Plasmas* **14** 082501

[29] Veshchev E.A. *et al* 2012 *Fusion Sci. Technol.* **61** 172

[30] Cauffman S. *et al* 1995 *Nucl. Fusion* **35** 1597

[31] Vayakis G. *et al* 2006 *Nucl. Fusion* **46** S836

[32] Crocker N.A. *et al* 2011 *Plasma Phys. Control. Fusion* **53** 105001

[33] Lamalle P. *et al* 2013 *Fusion Eng. Des.* **88** 517